Supplementary information (SI)

High performance biphasic Na_xMnO_2 electrode for low-cost and powerful aqueous sodium batteries and capacitors

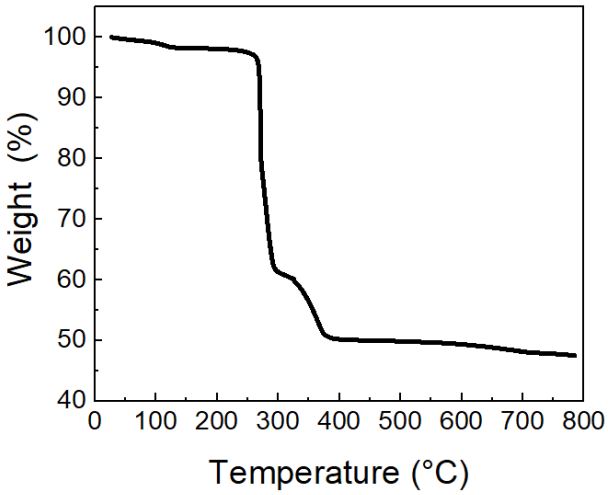

Figure S1. Differential thermal analysis (DTA) analysis.

TEM results

In the case of $NaMnO_2$ and $Na_{1.2}MnO_2$ samples, it is clear that FFTs shows the appearance of other diffraction spots near the observed ones in sample $Na_{0.8}MnO_2$.

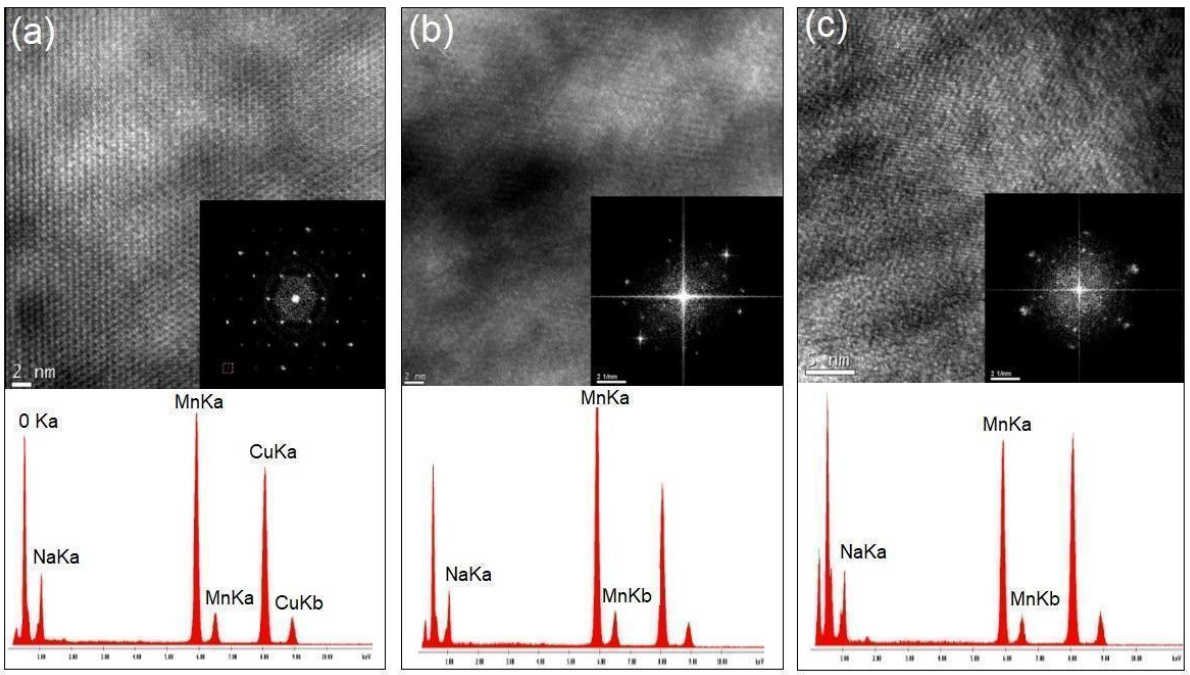

Figure S2. HRTEM images, its corresponding FFTs and EDX spectra for $Na_{0.8}MnO_2$ (a), $NaMnO_2$ (b) and $Na_{1.2}MnO_2$ (c).

These new diffraction spots are attributed to the monoclinic structure of Na_xMnO_2. High resolution TEM images demonstrated that sample $Na_{0.8}MnO_2$ is composed of only orthorhombic structure but in $NaMnO_2$ and $Na_{1.2}MnO_2$ both monoclinic and orthorhombic structures coexist. The experimental interplanar distance (d-values) and lattice parameters are in good agreement with the XRD results and are indexed as the orthorhombic phase (JCPDS:00-025-0844) with space group Pmm and monoclinic phase of $NaMnO_2$ (JCPDS: 01-073-0156) with space group C2/m.

$Na_{0.8}MnO_2$		$NaMnO_2$		$Na_{1.2}MnO_2$	
d_{hkl} (nm)	(hkl) /phases	d_{hkl} (nm)	(hkl)/ phases	d_{hkl} (nm)	(hkl) /phases
0.64	(001) ortho	0.65	(001) ortho	0.65	(001) ortho
0.24	(200)/(110) ortho	0.54	(001) mono	0.55	(001) mono
0.22	(200)/(012) ortho	0.24	(200)/(110)ortho &/or (-111)/(-202) mono	0.24	200)/(110) ortho &/or (-111)/(-202) mono
0.17	(013) ortho	0.21	(111) mono		
		0.14	(-400)/(-313)/ (-204)/(020)/(-402)/ (-401) mono		

Table S1. Interplanar distances extracted from SAED patterns for Na_xMnO_2

It is worth noticing that at this state, regarding the small difference between interplanar distances of different planes of different crystal system of $NaMnO_2$ (namely monoclinic and orthorhombic phases), it is very difficult to accurately assign the family plan to the measured interplanar distances. In table 1 are presented some interplanar distances extracted from SAED patterns of samples. EDX spectra of the prepared samples confirmed only the presence of Mn, Na and O and result in a pure Na_xMnO_2 compounds without any contaminations.

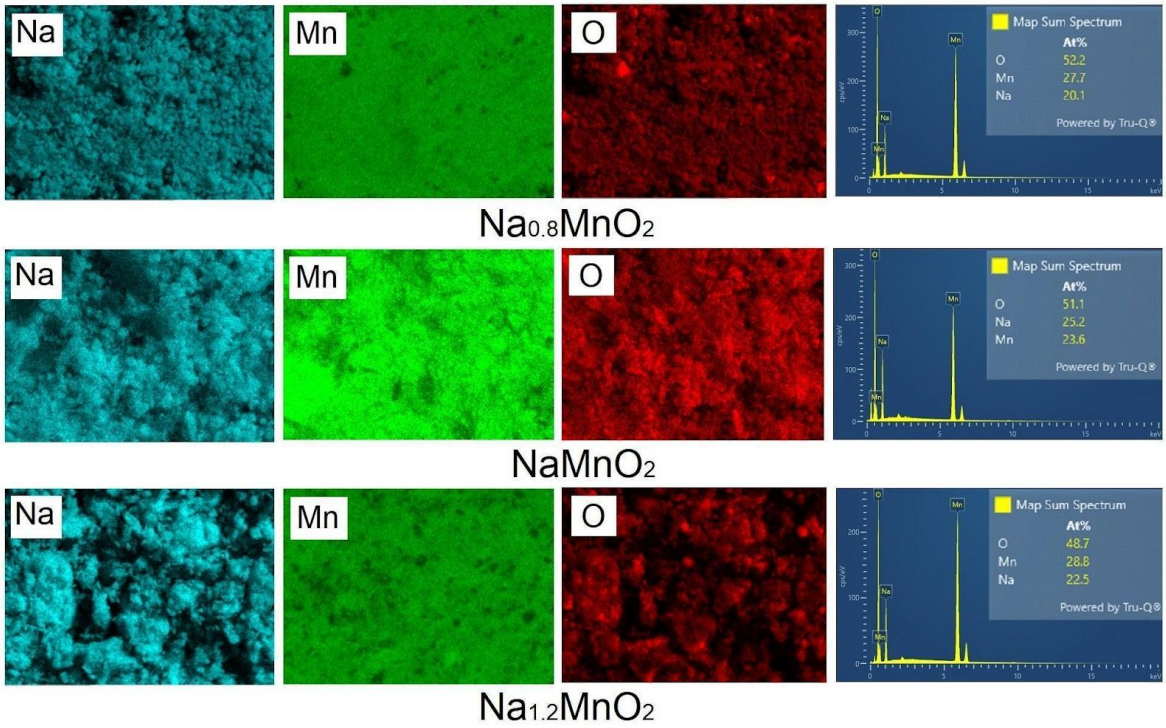

Figure S3. EDS maps of $Na_{0.8}MnO_2$, $NaMnO_2$ and $Na_{1.2}MnO_2$

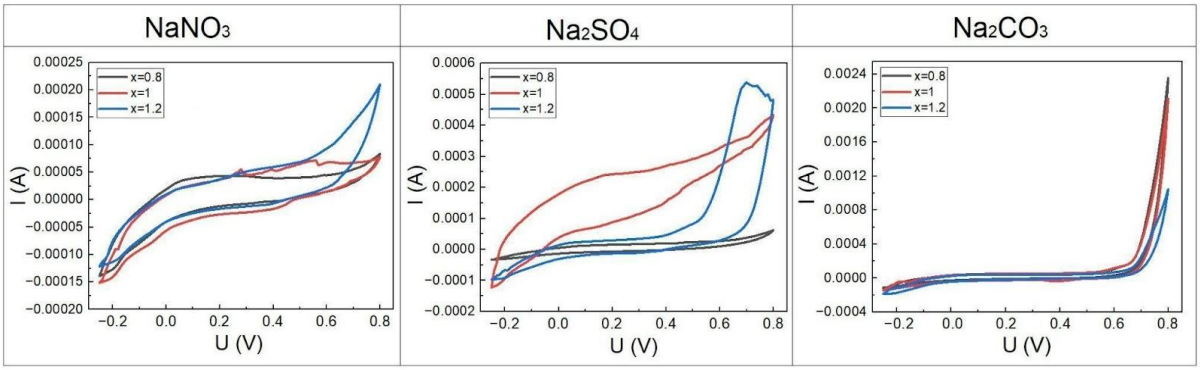

Figure S4. Cyclic voltammetry (CV) curves of $Na_{0.8}MnO_2$ (black), $NaMnO_2$ (red) and $Na_{1.2}MnO_2$ (blue) in different electrolytes at the scanning rate 0.5 mV/s.

Powder											
	Na 1s				**Mn 2p**			**O 1s**			
Sample	**Na^0 (%)**	**Na_xMnO_2 (%)**	**Na_2SO_4 (%)**	**Na-OH (%)**	**Mn^{+2} (%)**	**Mn^{+3} (%)**	**Mn^{+4} (%)**	**O-defects (%)**	**Mn-O-Mn (%)**	**Mn-OH (%)**	**H-O-H (%)**
X=1.2	62	38	0	0	26	46	28	18	68	2	12
X=1	0	100	0	0	32	26	42	7	54	10	29
X=0.8	35	65	0	0	30	8	62	8	64	9	19
After cycling											
	Na 1s				**Mn 2p**			**O 1s**			

Sample	Na^0 (%)	Na_xMnO_2 (%)	Na_2SO_4 (%)	Na-OH (%)	Mn^{+2} (%)	Mn^{+3} (%)	Mn^{+4} (%)	O-defects (%)	Mn-O-Mn (%)	Na-OH/ Mn-OH (%)	H-O-H (%)
X=1.2	0	56	26	18	4	26	70	0	29	36	35
X=1	0	25	40	34	2	8	91	0	16	53	31
X=0.8	0	58	3	39	5	25	70	0	30	33	37

Table S2 . Calculated atomic ratios of Na 1s, Mn 2p and O 1s components in samples $Na_{0.8}MnO_2$ (x=0.8), $NaMnO_2$ (x=1.0) and $Na_{1.2}MnO_2$ (x=1.2) before (Powder) and after cycling by consideration of core-level cross-sections at the used photon energy of high-resolution X-ray photon emission spectroscopy (XPS) analysis.

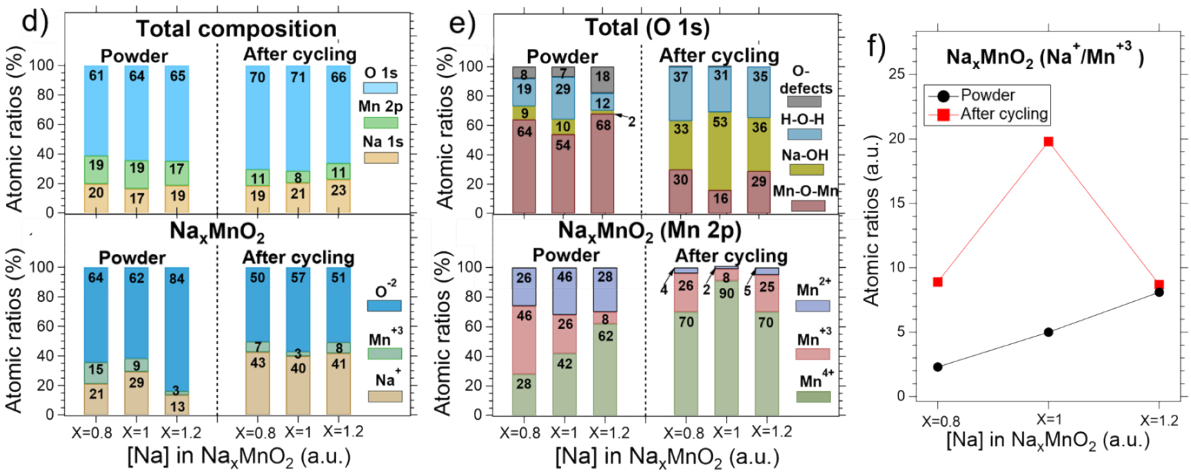

Figure S5. Calculated histogram of atomic O 1s, Mn 2p and Na 1s core-level element ratios in samples with x=0.8, x=1 and x=1.2 before and after cycling with a comparison of their total composition and composition just in the Na_xMnO_2 crystal, i. e., not including detected defects and amorphous phases (d), a histogram of total composition of atomic ratios in O 1s core-levels in samples before and after cycling (e-upper panel), and a histogram of Mn 2p core-levels of atomic element's composition just in the Na_xMnO_2 crystal in the samples before and after cycling (e-bottom panel). Calculated Na^+/Mn^{+3} atomic ratios just in the Na_xMnO_2 crystal in the samples before and after cycling (e), and Calculations were done by consideration of core-level cross-sections at the used photon energy.

We calculated Na, Mn and O atomic ratios of powder's surface composition by consideration of core-level cross-sections at the used photon energy (Fig.5d). The atomic percentage of total chemical composition (Figure 5d upper panel SI) agree with those measured by EDS (Fig.3 SI). By consideration of just chemical composition of ionic elements bounded in the Na_xMnO_2 powder crystal (Na^+ Mn^{3+} and O^{-2}), i.e., not-including non-ionic elements, amorphous components and defects (see Fig. 5d bottom panel), shows decreasing amount of Mn^{+3} oxidation state with increasing sodium amount. Calculated atomic Na^+/Mn^{+3} ratios depicted in Fig. 5f of the SI linearly increase with increasing sodium amount. Important finding is that the maximal amount of incorporated ionic sodium has been found in powders prepared with x=1 sodium concentration (see Fig. 5d bottom panel).

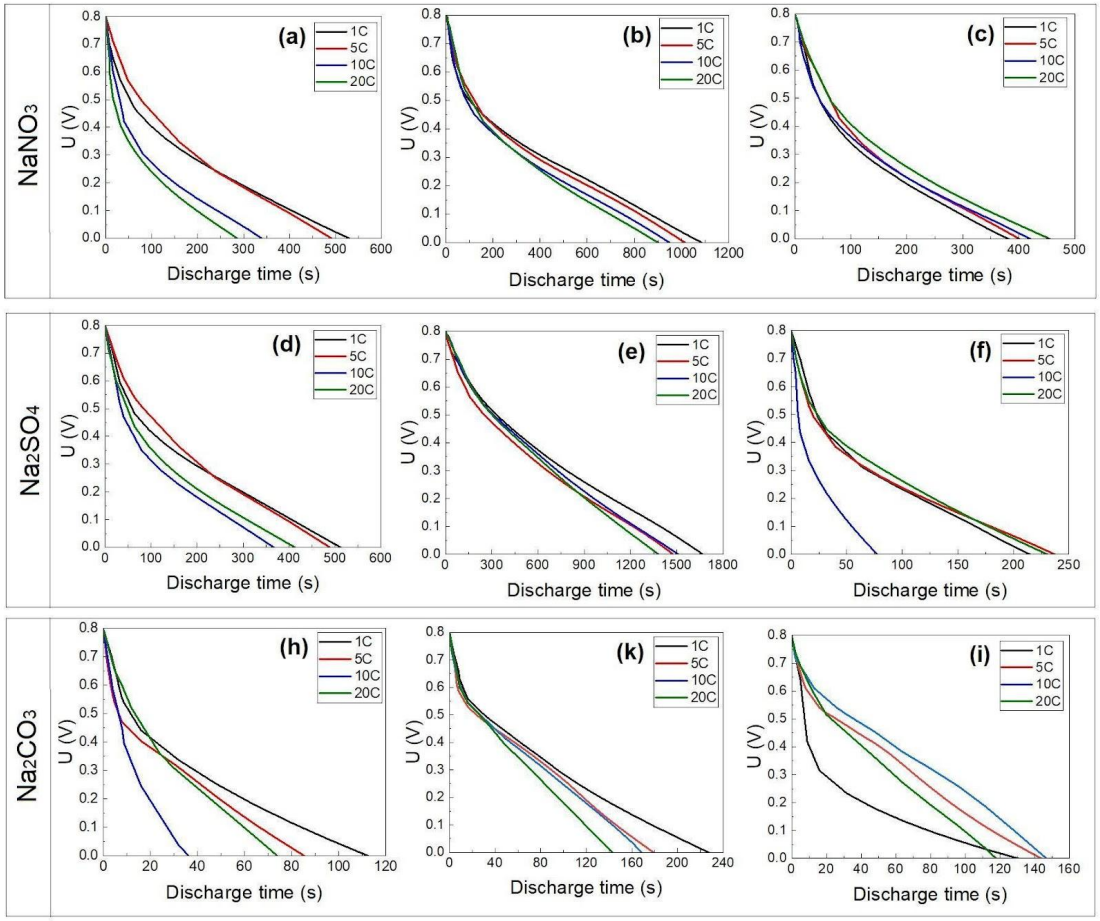

Figure S6. Discharge curves of $Na_{0.8}MnO_2$ (a, d, h), $NaMnO_2$ (b, e, k) and $Na_{1.2}MnO_2$ (c, f, i) in different electrolytes.

Explanation of our approach for diagram "capacity-power" building

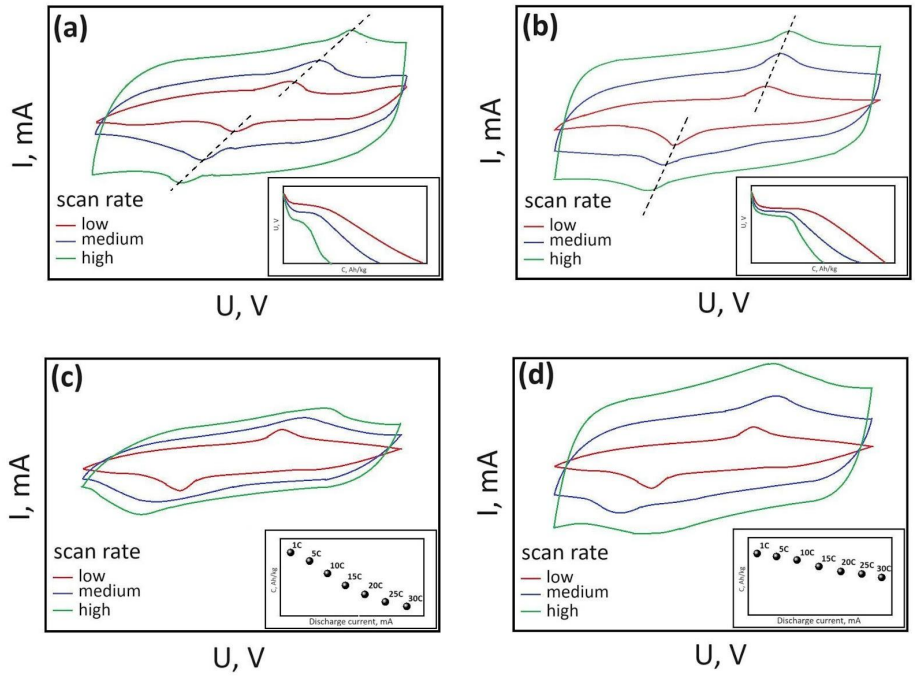

Figure S7. Example of CVA curves for electrode material with both pseudocapacity types - intercalation and absorption with bad (a) and good (b) high power ability, low (c) and high (d) capacity retention under high operating currents